

Reservoir modeling, rock physics, and seismic simulation of CO₂ sequestration in coal beds

*Dimitri Bevc**, Fusion Petroleum Technologies Inc., *Sergio E. Zarantonello*, Algorithmica LLC, *Jerry M. Harris*, Stanford University

Summary

We present results of an integrated simulation study to assess the effectiveness of surface seismic imaging for monitoring CO₂ sequestration. We considered two scenarios. In the first, injected CO₂ remained confined within a shallow coal formation. In the second, the sequestered CO₂ gas leaked through a semi-permeable shale layer to an overlying sand unit sealed above. The reservoir and seismic simulations required the construction of 3D geologic and facies models, the estimations of seismic velocities based on rock physics correlations, and the development of geostatistical dual-porosity reservoir descriptions of the coal and overlying shale and sand units. We ran the 3D reservoir simulations with an equation-of-state compositional reservoir simulator with the capability to model adsorption of injected CO₂ in coal, desorption of CH₄, and matrix shrinkage-swelling effects. We generated synthetic seismograms by simulating the propagation of acoustic waves through the 3D heterogeneous media, and used reverse time migration to create 3D seismic images corresponding to the state of the reservoir at the beginning and end of ten years of CO₂ injection. The resulting seismic images clearly identified the regions of CO₂ gas saturation, closely matching the gas saturation profiles predicted by the reservoir simulator.

Introduction

The injection and storage of captured CO₂ in coal beds has been considered as a strategy to reduce CO₂ emissions to the atmosphere, with the production of desorbed CH₄ (ECBM) partially covering the operational costs (Agrawal, 2003; Prusty, 2008). The acceptability of this and any other strategy for geologic storage of CO₂ depends on the ability to detect early leakage of CO₂ to overlying geologic units, and give enough lead time for the operators to lower the formation pressure before the gas reaches the surface. In this study we investigate the effectiveness of time-lapsed seismic imaging with reverse time migration (RTM) to monitor CO₂ injection and sequestration in shallow coal beds.

The underlying principle in time-lapsed seismic monitoring is that changes in the seismic impedance and velocity occur as the state of the reservoir changes. These changes are mostly caused by changes in the phase saturations, and to a lesser extent phase compositions and phase pressures in the pore space, which affect the constitutive properties and seismic wave propagation in the subsurface. The combined effect of pore saturations and pressures on seismic impedance is manifested by changes in seismic amplitude, whereas the effect on seismic velocity can be observed by changes in the seismic travel times. The most dramatic changes are in the amplitude of seismic waves when liquid pore fluids are replaced by gaseous-liquid mixtures (Majer et. al, 1997). A gaseous-liquid mixture has a high compressibility, as the gaseous phase, but a density similar to that of the liquid phase. This results in seismic velocities which may be lower than under pure liquid or pure gaseous saturating conditions. In particular, the amplitudes of waves reflected from the affected sedimentary layers may decrease by an order of magnitude. Changes of seismic travel-times are harder to observe because the thickness of the reservoir is generally small compared to its depth. However, the combination of travel-time and amplitude changes can be used to detect regions in the subsurface where changes in phase saturations occur (Kaelin and Johnson, 1999). Time-lapsed seismic surveys are designed to detect these changes over time. Seismic monitoring of CO₂ sequestration, or more generally of any reservoir process, is based on these principles.

The Geologic Reservoir Model

We developed a geologic and facies model approximately representing the Powder River Basin (PRB) and the Big George coal seam within the basin fill sediments. Based on the sandstone cross-beds, grain size, and grain shape distribution the PRB depositional environment is considered fluvial (Seeiand, 1992). This area was studied by Ross (2007), and our study incorporates parameters from her work. The Earth model is outlined in Fig. 1. It is a cube projecting from the surface of the Earth downward, to a depth of 435 m. Its areal dimensions are 990 m and 1080 m along in-line and across-line directions respectively. It represents a 5-spot injection-production pattern in Big George, with four producing wells at the corners and one injector in the center at an 80 acre inter-well spacing. In Fig. 1 the coal reservoir is shown black, a thin semi-permeable shale layer above is white, and the overlying sand unit is yellow. The overburden and underburden, not included in the reservoir model, are shades of gray. The geocellular grid has $435 \times 1080 \times 990 = 465,102,000$ cells. The cells (1 m in each edge) are too small to display in Fig. 1.

Seismic coal bed CO₂ sequestration monitoring

We assumed nine facies, each representing the aspect of the Earth model in an interval of geologic time. The nine facies in the Earth model shown in Fig. 1 are near flat sediments with varying proportions of sandstone, conglomerate, siltstone, limestone, and coal. The coal thickness was set at approximately 60 m throughout the model, about the maximum measured thickness of Big George coal.

Reservoir Simulation and Rock Physics

The 3D reservoir simulation model we used is a modification of a geostatistical dual-porosity reservoir model of Big George constructed by Ross (2007). The maximum thickness of the flow model was set to 100 m, with the coal bed itself reaching a thickness of 60 m (approximately the maximum thickness of Big George coal). We assumed a constant temperature of 22 °C and an initial pressure gradient of 7.12 kPa/m. In one of two simulated scenarios we included two vertical fractures that cut through the overlying shale which served as a partial seal. The assumption, in this case, was that the CO₂ leaked into the overlying sand but did not migrate through the layers above the sand. Throughout the ten-year simulated injection-production process, the CO₂ remained in gaseous or adsorbed phases (conversions to liquid or supercritical states did not occur). Total injected volumes of CO₂, referenced to standard pressure and temperature conditions, were between 8×10^7 m³ and 9×10^7 m³ in the two scenarios. Injection rate was constrained by specified bottom hole pressure and maximum pipe capacity. Injection rates remained roughly constant in the two scenarios. The production wells produced about 7×10^4 m³ of methane co-produced with approximately 5×10^5 m³ of water.

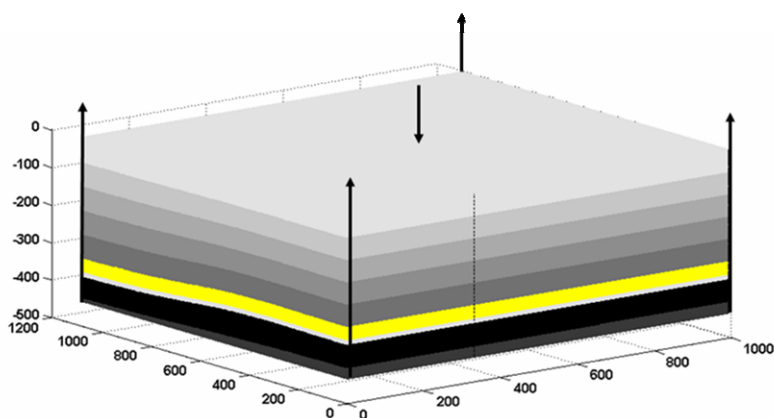


Figure 1. Geocellular Earth model of 5-spot pattern for coal bed CO₂ injection.

We ran our flow simulations with GEM, an equation-of-state compositional reservoir simulator from Computer Modelling Group. GEM is an industry standard ECBM simulator, featuring: (1) extended Langmuir Isotherms to model the preferential adsorption of CO₂, and (2) models for coal shrinkage and swelling and their effect on matrix permeability and porosity. The resulting flow simulations represented a ten-year CO₂ injection and sequestration process.

Following reservoir modelling, rock physics relationships are used to estimate acoustic impedance: i.e. seismic wave velocity and rock density. These parameters will vary with porosity, fluid saturation, and lithology. In our study we used rock physics correlations to build three P-wave velocity models:

- Baseline model representing acoustic velocity before CO₂ injection.
- Velocity model for the CO₂ leakage scenario after ten-years of CO₂ injection process.
- Velocity model for the non-leakage scenario after ten years of CO₂ injection.

We used Batzle-Wang relations to estimate acoustic velocity in fluids, Gassman's fluid substitution model for the effects of saturating fluids on rock bulk moduli, and correlations of Dvorkin and Mukerji (personal communication) for the elastic properties of the rock matrix. The density and bulk modulus of brine were assumed constant, while those of CO₂ and CH₄ varied strongly with pressure. For CO₂ density and bulk modulus we used the specific correlation of Batzle and Wang (1992). The P-wave velocities in the coal zone of our baseline model (average $V_p = 2700$ m/s, average depth = 370 m) were higher but comparable to values derived from bore-hole sonic measurements (Flores, 2004) of the nearby but shallower Knobloch and Flores-Goodale coal basins (average $V_p = 2200$ m/s, average depth = 150 m).

Seismic coal bed CO₂ sequestration monitoring

Seismic Modeling and Imaging

3-D acoustic modelling was used to create synthetic seismograms corresponding to the beginning and end of the simulated ten-year CO₂ injection process. These calculations were run with an explicit finite-difference solver for the wave equation in a heterogeneous medium. For imaging, we chose RTM because of its ability to image steep dips and recumbent surfaces. We deployed a dense regular arrangement of shots and receivers, with 40m spacing between shot locations to provide a high spatially sampled measure of the subsurface reflectivity. The distance between receivers was set at 10 m. An 80 Hz Ricker wavelet was used for the wave equation modeling, and frequencies up to 80 Hz were migrated with RTM. The Rayleigh limit of resolution is defined to be 1/4 of the dominant wavelength. Given a dominant frequency of about 40 Hz, and propagation velocity of about 2800 m/s at the target zone, this yields a resolution of about 17.5m. A frequency of 80 Hz would give about 8m resolution, but the deeper the target, the more high frequencies are attenuated. Further studies are planned to decimate the number of surface shot and receiver locations, thereby reducing cost, and potentially increasing temporal resolution for CO₂ monitoring, accounting, and validation.

Results

In this study we focused on the correlation between the seismic images created with RTM and the gas saturations obtained from flow simulations using GEM. We considered CO₂ leakage (case 1) and non-leakage (case 2) scenarios. In all cases the RTM images correlated closely with the CO₂ gas saturation profiles. As an example, in Figures 2 (top) we show inline sections of the seismic image volume before injection, and in Figure 2 (bottom) we show the same sections at the end of ten years of CO₂ injection showing gas accumulations under both, primary and secondary seals.

In Figure 3 we show inline sections of P-wave velocity (top) and gas saturation (bottom). Although the primary factor affecting acoustic velocity is the saturation of the injected CO₂ gas, there are detectable effects in the seismic image caused by factors other than gas saturation, such as mineral content and rock type of the geological facies, variable porosity and pressure, and variable compositions of saturating fluids (brine, coal gas, and injected gas).

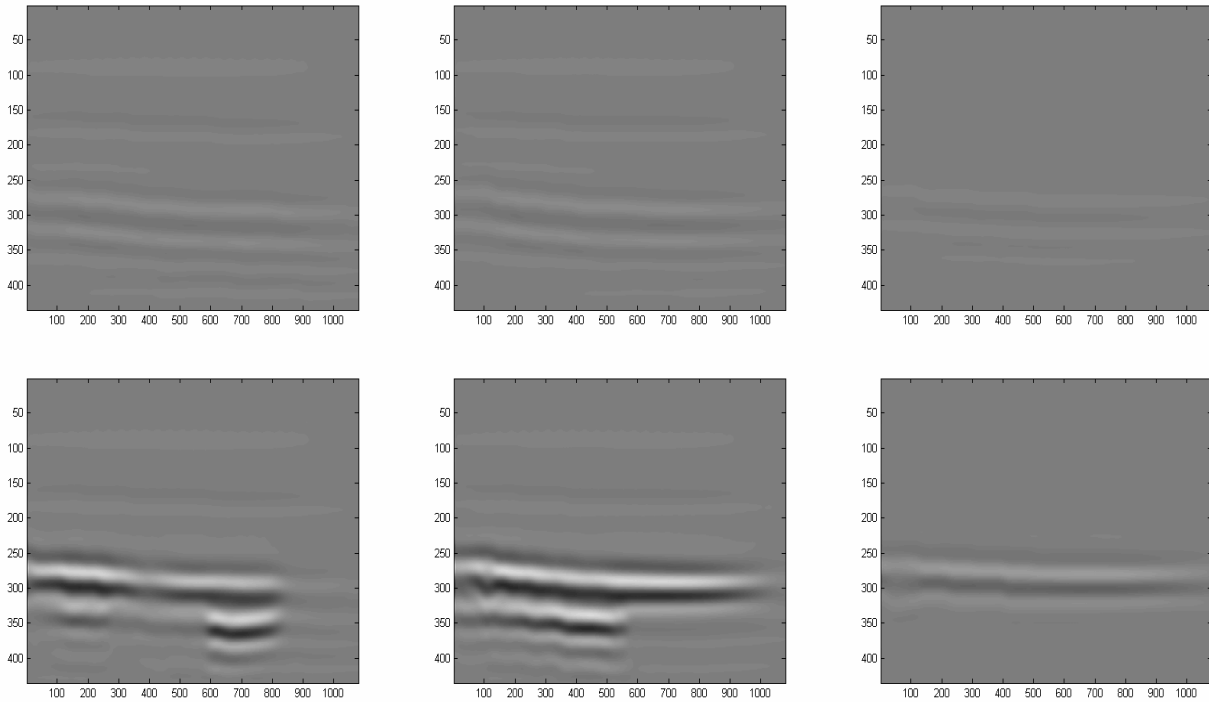


Figure 2. Cross-sections (from left to right: inline = 330m, 660m, 990m). Seismic depth images before CO₂ injection (top), and after 10 years of CO₂ injection (bottom).

Seismic coal bed CO₂ sequestration monitoring

Conclusions

The consistency of results obtained with special-purpose reservoir simulation, rock physics, and seismic imaging, validate the applicability of seismic imaging as a monitoring tool for geologic CO₂ storage. While it may not be practical to deploy spatially dense seismic surveys for CO₂ monitoring, verification, and assessment in all field operations, this study provides high-quality images that can serve as standards for comparison with other methods, and assist in the development and fine-tuning of less expensive monitoring procedures. One area we did not address was how to distinguish the seismic signatures of CO₂ and CH₄ gas. Additional research is necessary to define an integrated reservoir simulation, rock physics, and seismic imaging workflow providing an advanced monitoring capability for CO₂ sequestration. This study is a first step toward this goal.

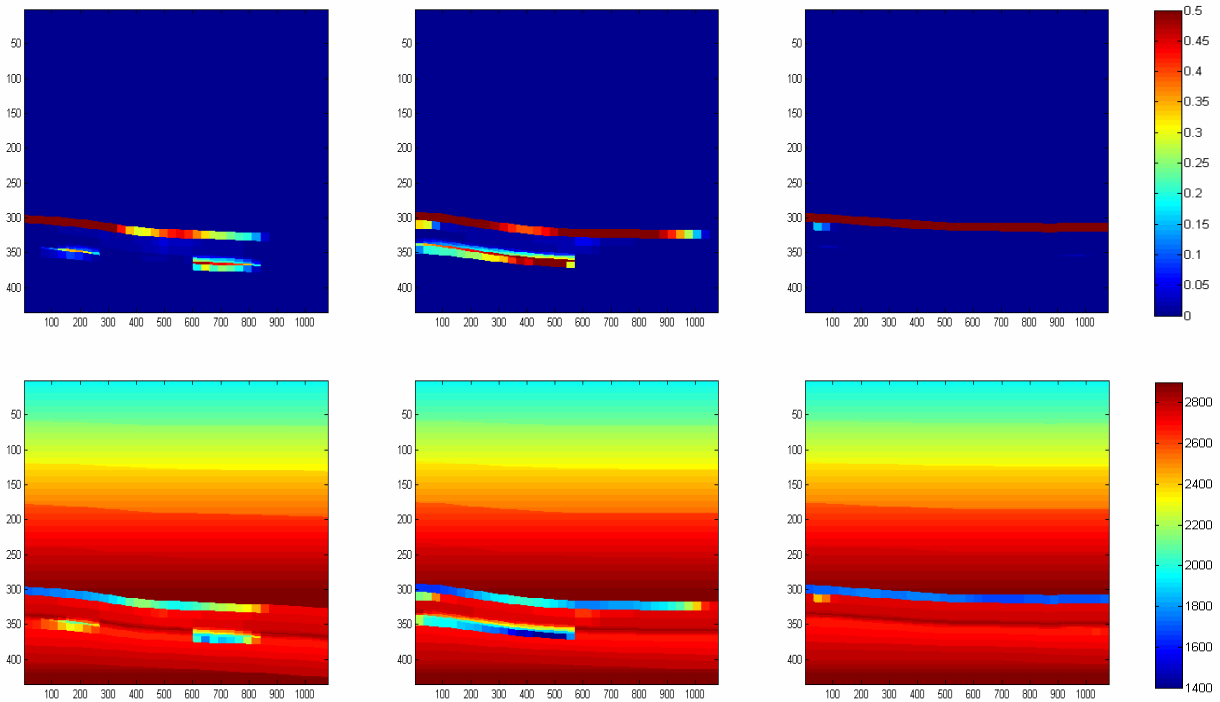


Figure 3. Cross-sections (from left to right: inline = 330m, 660m, 990m) after 10 years of CO₂ injection. P-wave velocity m/s (bottom), CO₂ gas saturation (top).

Acknowledgements

The authors thank Y. Quan, T. Mukerji, J. Dvorkin, and B. Kaelin for their advice and input. The research was supported by the U.S. D.O.E. through Agreement No. DE-FG02-06ER86263.